Cancer Chemother Pharmacol (2011) 68:227–238
DOI 10.1007/s00280-010-1477-8

ORIGINAL ARTICLE

Inhibition of *N*-linked glycosylation by tunicamycin induces E-cadherin-mediated cell–cell adhesion and inhibits cell proliferation in undifferentiated human colon cancer cells

Julio Cesar Madureira de Freitas Junior · Bárbara Du Rocher D'Aguiar Silva · Waldemir Fernandes de Souza · Wallace Martins de Araújo · Eliana Saul Furquim Werneck Abdelhay · José Andrés Morgado-Díaz

Received: 6 July 2010 / Accepted: 21 September 2010 / Published online: 7 October 2010

Abstract
Purpose Aberrant protein glycosylation and disassembly of E-cadherin-mediated cell–cell adhesion are characteristics of epithelial cancer. However, the relationship between these two events in colorectal cancer remains to be defined. In this study, we analyzed whether *N*-glycan expression is crucial for the loss of E-cadherin-mediated cell–cell adhesion in human colorectal cancer cells.
Methods Differentiated Caco-2 and undifferentiated HCT-116 colon cancer cells were used as models of stable and unstable adherens junctions (AJs), respectively. Complex-type *N*-glycans were detected using the lectins E-PHA (*Phaseolus vulgaris* E.) and L-PHA (*Phaseolus vulgaris* L.). To study E-cadherin-mediated AJ assembly, we examined the effects of swainsonine, an inhibitor of α-mannosidase II, and tunicamycin, a drug that inhibits the biosynthesis of *N*-glycans, via western blot, immunofluorescence, differential extraction in Triton X-100, and electron microscopy. Cell proliferation and apoptosis were examined by crystal violet staining and flow cytometry, respectively.
Results We observed positive labeling for E-PHA and L-PHA lectins in both cell lines; however, HCT-116 cells had increased E-cadherin-linked complex-type *N*-glycans. Interestingly, tunicamycin, but not swainsonine, was able to induce functional E-cadherin-mediated cell–cell adhesion in undifferentiated HCT-116 cells, as shown by the increased association of E-cadherin with the actin cytoskeleton. Moreover, in HCT-116 cells, tunicamycin also induced the formation of tight cell–cell contacts, and it inhibited cell proliferation without triggering apoptosis.
Conclusions Collectively, our results demonstrate for the first time that altered *N*-glycan expression plays an important role in the loss of AJ stability in undifferentiated colorectal cancer cells and that this loss may be associated with the progression of colorectal cancer.

Keywords Tunicamycin · Swainsonine · Colorectal cancer · Adherens junctions · E-cadherin · *N*-glycosylation

J. C. M. de Freitas Junior · W. F. de Souza · W. M. de Araújo · J. A. Morgado-Díaz (✉)
Divisão de Biologia Celular, Coordenação de Pesquisa, Instituto Nacional de Câncer, 37 André Cavalcanti street, 5th floor, Rio de Janeiro, RJ CEP 20230-051, Brazil
e-mail: jmorgado@inca.gov.br

B. D. R. D'AguiarSilva · E. S. F. W. Abdelhay
Centro de Transplante de Medula Óssea, Instituto Nacional de Câncer, 23 Cruz Vermelha square, 6th floor, Rio de Janeiro, RJ CEP 20230-130, Brazil

Introduction

Colorectal cancer (CRC) is among the most common human neoplasms. It is the third most frequent cancer worldwide, with an estimated one million new cases and half a million deaths each year [1]. In Brazil, it is also the third most common cancer, according to recent data from the *Instituto Nacional de Câncer* [2]. The progression of CRC is characterized by a series of clinical and histopathological stages [3], which range from single-crypt lesions, through small benign tumors (adenomatous polyps), to malignant cancers (carcinomas); in this final stage, the disruption of adherens junctions (AJs) is frequently observed [4]. AJs and tight junctions (TJs) constitute the apical junctional complex, which is responsible for maintaining the epithelial architecture [5]. AJs are dynamic multiprotein complexes in which E-cadherin, a transmembrane glycoprotein and the main mediator of cell–cell adhesion in the epithelium, is

anchored to the actin cytoskeleton via proteins of the catenin family [6].

The disassembly of AJs in CRC cells involves many pathways, including PI3K, Wnt, ERK1/2, and PKA, as well as pro-inflammatory signaling [7–11]. However, the role of post-translational protein modifications in this process is not yet clear. In CRC cells, our group showed that increased metastatic potential is correlated with changes in glycan expression [12]. In breast cancer cells, modulation of cell–cell and cell–matrix adhesion are associated with changes in glycan expression; the biological functions of cadherins and integrins can be modified by the presence of different glycan patterns on these molecules [13, 14]. E-cadherin can be post-translationally modified by phosphorylation, *O*-glycosylation, and *N*-glycosylation. For instance, in mouse NIH3T3 cells, casein kinase II phosphorylates the cytosolic tail of E-cadherin, which enhances its binding to β-catenin [15]. During apoptosis induced by endoplasmic reticulum stress, cytoplasmic *O*-glycosylation of the E-cadherin cytosolic tail prevents its transport to the cell membrane in MCF-7, MDA-MB-468, and MDCK cells [16]. Extensive modification of E-cadherin with complex-type *N*-glycans leads to the formation of dynamic but weak AJs, whereas its diminished *N*-glycosylation promotes the establishment of a stable assembly of AJs and TJs in MDCK cells [17, 18]. Recently, it was shown that in mammary carcinoma, *N*-glycosylated E-cadherin is characterized by highly branched *N*-glycans, increased sialylation and the expression of a few high-mannose structures [19].

N-Glycan biosynthesis can be blocked with pharmacological tools, such as swainsonine or tunicamycin. Swainsonine inhibits the α-mannosidase II enzyme, thereby blocking the formation of complex-type *N*-glycans [20]; tunicamycin blocks *N*-glycan biosynthesis by inhibiting the formation of a lipid-linked oligosaccharide precursor [21]. Agents that modulate carbohydrates expression have promising therapeutic potential for various cancers [22]. A Phase II clinical trial has used swainsonine as a therapeutic agent for renal cancer [23]. Recently, encouraging results have shown that tunicamycin enhances erlotinib-induced inhibition of cell growth in non-small-cell lung cancer cells [24]. Nevertheless, the role that E-cadherin glycosylation changes may play during CRC progression has not been explored.

In the present study, we investigated how changes in the expression of E-cadherin-linked *N*-glycans affect the stability of AJs in CRC cells. We showed that the instability of AJs correlates with an increase in *N*-glycosylated E-cadherin; these changes may contribute to CRC progression. Moreover, treatment with tunicamycin, but not swainsonine, induced functional E-cadherin-mediated cell–cell adhesion in undifferentiated HCT-116 cells, as shown by the increased association of E-cadherin with the actin cytoskeleton. Additionally, tunicamycin induced the formation of tight cell–cell contacts and inhibited the proliferation of HCT-116 cells without causing apoptosis. Our findings also support the use of tunicamycin as a chemotherapeutic agent in experimental models of CRC progression.

Materials and methods

Chemicals and antibodies

Mouse monoclonal anti-E-cadherin (36 clones) was obtained from BD Biosciences (San Diego, CA, USA), rabbit monoclonal anti-α- and anti-β-catenin were purchased from Sigma Chemical Co. (St Louis, MO, USA), and mouse monoclonal anti-β-tubulin was purchased from Zymed Laboratories Inc. (South San Francisco, CA, USA). Fluorescein- and peroxidase-conjugated anti-rabbit and anti-mouse IgG were purchased from Sigma Chemical Co. Agarose- and fluorescein-conjugated lectins L-PHA (*Phaseolus vulgaris* L.—Leukoagglutinating) and E-PHA (*Phaseolus vulgaris* E.—Erythroagglutinating) (Table 1) were purchased from United States Biological (Swampscott, MA, USA). The drugs tunicamycin (A1 homolog) and swainsonine were obtained from Sigma Chemical Co.

Cell culture

Caco-2, a differentiated cell line with moderate invasive potential derived from colon adenocarcinoma, and HCT-116, an undifferentiated and very invasive cell line derived from colon carcinoma [25–27], were obtained from the American Type Culture Collection (ATCC; Manassas, VA, USA). Cells were cultured at 37°C in a humidified atmosphere of 5% CO_2/air in DMEM (GIBCO—Invitrogen, USA) supplemented with 10% heat-inactivated fetal bovine serum (GIBCO), penicillin G (60 mg/l), and streptomycin (100 mg/l). For experimental purposes, cells were plated on culture flasks, plates, glass coverslips, or on

Table 1 Specificities of lectins used in this study

Lectins	Specificities
E-PHA (*Phaseolus vulgaris*—Erythroagglutinating)	Bisected di- and triantennary complex-type *N*-glycans with β-1,4-linked *N*-acetylglucosamine [39]
L-PHA (*Phaseolus vulgaris*—Leukoagglutinating)	Tri- and tetraantennary complex-type *N*-glycans with β-1,6-linked *N*-acetylglucosamine [36]

Transwell polycarbonate filters with a 0.4-μm pore size (Costar, Cambridge, MA).

Total cell lysates and differential extraction in Triton X-100

Total cell lysates were obtained by incubating the cells in lysis buffer [1% Triton X-100, 0.5% sodium deoxycolate, 0.2% SDS, 150 mM NaCl, 2 mM EDTA, 10 mM Hepes (pH 7.4), 20 mM NaF, 1 mM orthovanadate and a protease inhibitor cocktail (1:100 dilution)], for 30 min at 4°C. After centrifugation at 10,000*g* for 10 min at 4°C, the supernatant was removed and stored at −20°C for subsequent analysis.

For differential cell extraction in Triton X-100, samples were rinsed three times in phosphate-buffered saline (PBS) and incubated for 20 min at 4°C in cytoskeletal (CSK) extraction buffer [50 mM NaCl, 10 mM Pipes (pH 6.8), 3 mM $MgCl_2$, 0.5% Triton X-100, 300 mM sucrose, 1 mM orthovanadate, 20 mM NaF, and protease inhibitors]. Cells were scraped from plates, homogenized, and centrifuged at 10,000*g* for 10 min at 4°C. The supernatant corresponding to the Triton X-100-soluble fraction (actin cytoskeleton-unlinked proteins) was removed and stored at −20°C. The pellet was resuspended in SDS buffer [20 mM Tris–HCl (pH 7.5), 5 mM EDTA, 2.5 mM EGTA, 1% SDS] and boiled at 100°C for 10 min. After centrifugation for 10 min at 10,000*g*, the supernatant, corresponding to the Triton X-100-insoluble fraction (actin cytoskeleton-linked proteins), was gently removed and stored at −20°C.

Western blot

Equal amounts of protein (30 μg/lane) from total cell lysates and Triton X-100 cell fractions were separated on 10% SDS–PAGE and transferred onto nitrocellulose sheets. The membranes were blocked and incubated overnight with primary antibodies to selected proteins. After washing, the membranes were incubated for 1 h with peroxidase-conjugated secondary antibodies, and proteins were visualized using an enhanced Amersham Biosciences GE chemiluminescence kit (Buckinghamshire, UK). Band images were quantified by optical density using LabWorks 4.6 software (UVP Inc., Upland, CA, USA).

Analysis of lectin labeling by flow cytometry

Cells were washed, collected from plates, and then centrifuged at 1500 g for 3 min; the precipitate was resuspended in 100 μl of PBS. FITC-conjugated (fluorescein isothiocyanate) E-PHA or L-PHA lectins were added at a final concentration of 50 μg/ml. After incubation for 20 min at room temperature, the cells were collected by centrifugation, washed three times with PBS, and fixed in a solution containing 4% paraformaldehyde. Cells were analyzed by flow cytometry (FASCalibur, Becton–Dickinson, Mountain View, CA), with unstained cells serving as controls. Fluorescence histograms and mean fluorescence data were created and analyzed with CellQuest software (Becton–Dickinson).

Agarose–lectin precipitation assay

Equal amounts of protein (500 μg) from total cell lysates were adjusted to a final volume of 600 μl and incubated with 50 μl of a suspension containing agarose-conjugated lectins (50 μg of L-PHA or 50 μg of E-PHA) for 2 h at 4°C in an orbital shaker. After the agarose beads were precipitated by centrifugation at 10,000*g* for 30 s, the supernatant was removed, and the beads were washed three times with 500 μl of lysis buffer. The beads were resuspended in 30 μl of sample buffer [28] and boiled for 5 min prior to analysis by lectin blotting and western blotting for E-cadherin.

Treatment with *N*-glycosylation inhibitors

Tunicamycin and swainsonine stock solutions were diluted in culture medium (DMEM) supplemented with 10% heat-inactivated fetal bovine serum to final concentrations of 1 or 2 μg/ml for swainsonine and 1 μg/ml for tunicamycin [14, 29]. After reaching 80% confluence, cells were treated with the drugs for 24 h and prepared for subsequent analysis. A low calcium (LC) condition was obtained by the addition of EDTA (4 μM) in the culture medium for 30 min.

Confocal microscopy

For analysis of lectins by fluorescence microscopy, cells grown on sterile coverslips were washed three times with PBS supplemented with 100 mM $CaCl_2$ and 100 mM $MgCl_2$ (PBS/CM), fixed in a solution containing 4% paraformaldehyde for 10 min, and permeabilized with 0.1% Triton X-100. Cells were then washed in PBS/CM and incubated with a solution containing 50 mM NH_4Cl. Subsequently, they were washed and incubated in a blocking solution (0.3% BSA in PBS/CM) for 1 h, followed by an additional 1 h with FITC-conjugated L-PHA and E-PHA lectins. Finally, the coverslips were washed in PBS and mounted using n-propyl gallate. Cell staining was detected with a LSM 510 confocal microscope (Carl Zeiss Inc., Germany) equipped with LSM Image browser software.

For immunofluorescence analysis, the cells were fixed, permeabilized, and blocked as described earlier before being incubated with primary antibodies (anti-E-cadherin, anti-α-catenin and anti-β-catenin) for 1 h and FITC-

conjugated secondary antibodies for another 1 h. Finally, the cover slips were washed in PBS and mounted using *n*-propyl gallate. Cell labeling was detected with a LSM 510 confocal microscope. Images shown are representative of at least three independent experiments and were obtained using identical sensitivity parameters.

Transmission electron microscopy

Cells were cultured on Transwell polycarbonate filters (0.4 μm pore size and 0.33 cm^2 surface area; Corning Life Sciences, Lowell, MA) and fixed for 60 min in a solution containing 2.5% glutaraldehyde, 1% freshly prepared paraformaldehyde, 8% sucrose, and 2 mM $CaCl_2$. After two 10-min washes in 0.1 M cacodylate buffer, cells were post-fixed with 1% OsO_4 solution for 45 min. Then, monolayers were washed with cacodylate buffer, dehydrated with acetone series, and embedded in Epon resin. Ultrathin sections (70 nm) were stained with lead citrate and observed with a Zeiss CEM-900 transmission electron microscope (Carl Zeiss Inc., Germany).

Apoptosis analysis

Cells were grown in 12-well plates and treated for 24 h with tunicamycin or swainsonine. Cells were then trypsinized, washed, and resuspended in 1× binding buffer (10 mM HEPES/NaOH, pH 7.4; 140 mM NaCl; 2.5 mM $CaCl_2$) before being incubated with FITC-conjugated Annexin V (BD Biosciences) for 20 min at room temperature. Prior to flow cytometric analysis, 50 μg/ml of the vital dye propidium iodide (PI) was added to the cells. Cells were analyzed with a FASCalibur flow cytometer (FACScan, Becton–Dickinson, CA, USA) and CellQuest software (Becton–Dickinson).

Cell proliferation assay

The crystal violet method was used to measure cell proliferation. Cells (3×10^4) were cultured on 96-well plates for 0, 6, 18, and 24 h before being fixed with ethanol for 10 min. A crystal violet solution (0.05% crystal violet and 20% methanol) was added for 10 min. Cells were washed twice with water and then solubilized with methanol. The absorbance at 595 nm was measured with a Spectra Max 190 spectrophotometer (Molecular Devices, Sunnyvale, CA, USA).

Densitometric and statistical analysis

Student's *t* tests and one-way ANOVA were performed with GraphPad Prism 4.02 software (GraphPad Software Inc., San Diego, CA, USA). We considered data from three independent experiments to be statistically significant at $P < 0.05$. Graphic data are presented as the means + SEM.

Results

AJs are stable in differentiated Caco-2 cells but unstable in undifferentiated HCT-116 cells

To determine whether differentiated Caco-2 and undifferentiated HCT-116 cells could be used as models of stable and unstable AJs, respectively, we examined the subcellular localization of E-cadherin and α- and β-catenin by confocal microscopy. In Caco-2 cells, the distribution of AJ proteins (E-cadherin, α- and β-catenin) was restricted to cell–cell contact regions and very little cytoplasmic labeling appeared; in HCT-116 cells, however, stronger cytoplasmic labeling and a discontinuous cell–cell contact area were more evident (Fig. 1a). Next, the expression levels of AJ proteins were determined by western blot. As shown in Fig. 1b, HCT-116 cells expressed significantly ($P < 0.05$) lower levels of E-cadherin and α-catenin than did Caco-2 cells. In contrast, HCT-116 cells expressed higher levels of β-catenin, a finding that is consistent with the role of this protein during CRC progression [30]. We also evaluated the association of the actin cytoskeleton with E-cadherin and α- and β-catenin in these two cell lines, using Triton X-100 solubility criteria [31] and western blot analysis. Figure 1c shows that these associations were significantly ($P < 0.05$) lower in HCT-116 than in Caco-2 cells. Together, these data show that undifferentiated HCT-116 cells develop non-functional and unstable AJs; in contrast, differentiated Caco-2 cells possess functional and more stable AJs.

Glycans that react with E-PHA and L-PHA are increased in E-cadherin from unstable AJs

To determine whether Caco-2 and HCT-116 cells react positively with the lectins E-PHA and L-PHA (Table 1), we used a fluorescence assay to evaluate the presence of binding glycans recognized by these lectins. Although both cell lines reacted positively with the lectins (Fig. 2a), we observed a differential pattern of staining: in HCT-116 cells, labeled L-PHA was able to access the cell–cell contact areas, but in Caco-2 cells, the labeling was mostly localized at the apical region (Fig. 2a). These results suggest an increased *N*-glycan expression at cell–cell contact regions in HCT-116 cells; alternatively changes in cell–cell adhesion may allow L-PHA greater access to ligands in these cell regions. These data are more evident when analyzed in the X–Z plane. Both cell lines stained with

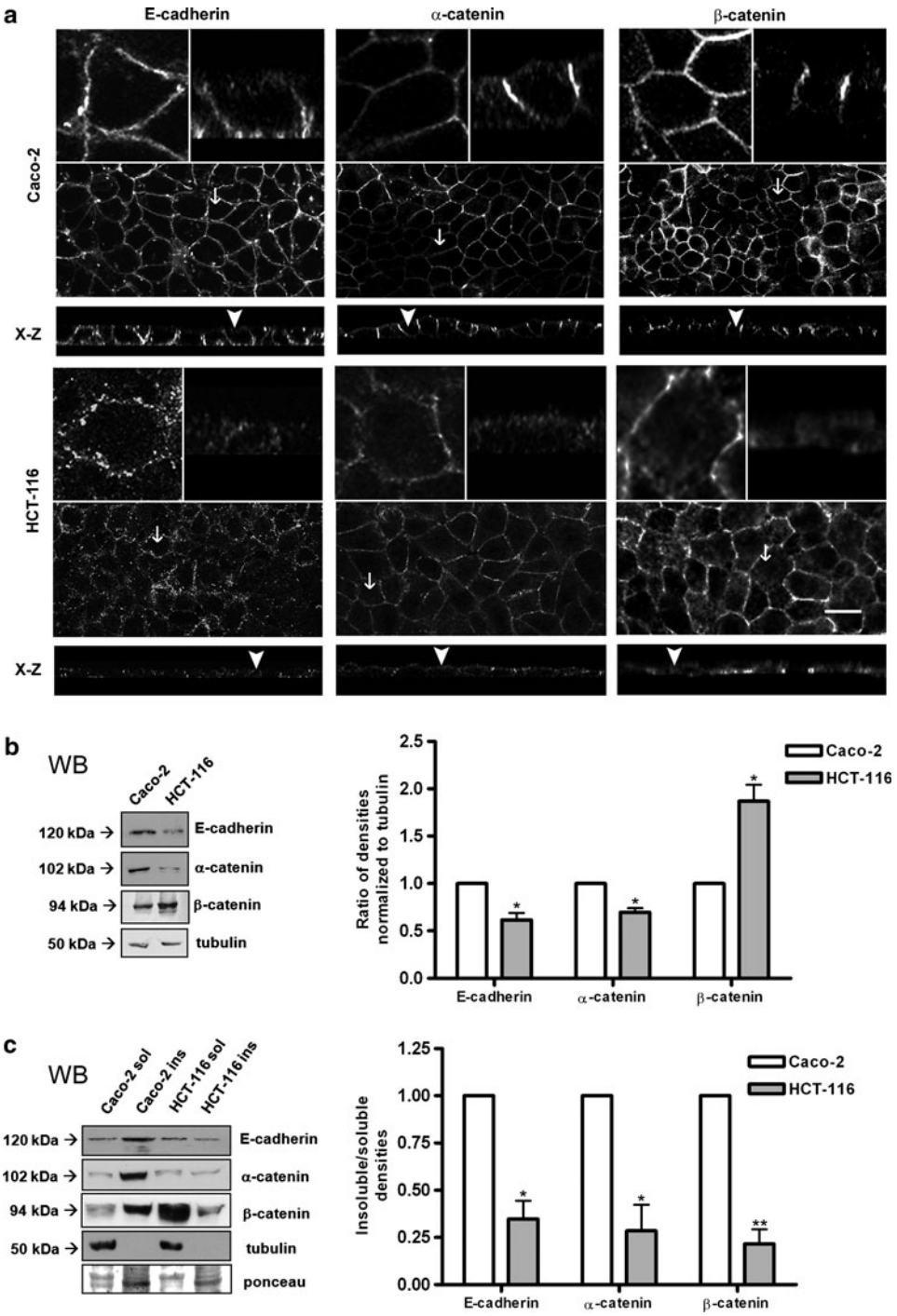

Fig. 1 Although differentiated Caco-2 cells develop stable AJs, these structures are unstable in undifferentiated HCT-116 cells. **a** Subcellular localization of AJ proteins in Caco-2 and HCT-116 cells. Cell monolayers were fixed and stained for E-cadherin and α- and β-catenins. Representative images obtained by confocal microscopy show a differential labeling pattern in the two cell lines. On the superior part of each *panel*, *arrows* and *arrowheads* indicate magnified images at the X–Y and Z–Y plane, respectively. *Bar* = 20 μm. **b** Differential expression of AJ proteins in Caco-2 and HCT-116 cells. Total lysates were obtained and the levels of E-cadherin and α- and β-catenins were detected by western blot. The *bar* graph shows the levels of AJ proteins; α-tubulin was used as a loading control. *Error bars* indicate means + SEM ($n = 3$). * $P < 0.05$. **c** Association of AJ proteins with the actin cytoskeleton in Caco-2 and HCT-116**.** Triton X-100 soluble and insoluble fractions (unassociated and associated with the cytoskeleton, respectively) were obtained as described in the "Materials and methods" section, and the levels of E-cadherin and α- and β-catenin were detected by western blot. The *bar* graph shows the relative amount of AJ proteins associated with the cytoskeleton. Both α-tubulin levels and Ponceau staining were used as loading controls. Error bars indicate means + SEM ($n = 3$). * $P < 0.05$; ** $P < 0.01$, Student's *t* test. *WB* western blot, *sol* soluble, *ins* insoluble

E-PHA showed a similar pattern at the supranuclear region; however, the staining was stronger in Caco-2 cells (Fig. 2a). To confirm that the cell-surface membranes of Caco-2 and HCT-116 cells also react positively with E-PHA and L-PHA, both cell lines were incubated with these lectins and the labeling was analyzed by flow cytometry. We observed a similar positive reaction in both cell lines (Fig. 2b, c). We therefore investigated whether the expression of E-cadherin-linked complex-type *N*-glycans correlated with the stability of the AJs. When we performed an agarose–lectin precipitation assay, followed by western blot for E-cadherin, we observed that HCT-116 cells exhibit an increase in the binding of E-PHA and L-PHA to E-cadherin, compared with Caco-2 cells (Fig. 2d). Because the two cell lines have opposite phenotypes in relation to AJ stability, these results indicate that increased *N*-glycosylation on the E-cadherin molecule correlates with AJ instability in CRC cells.

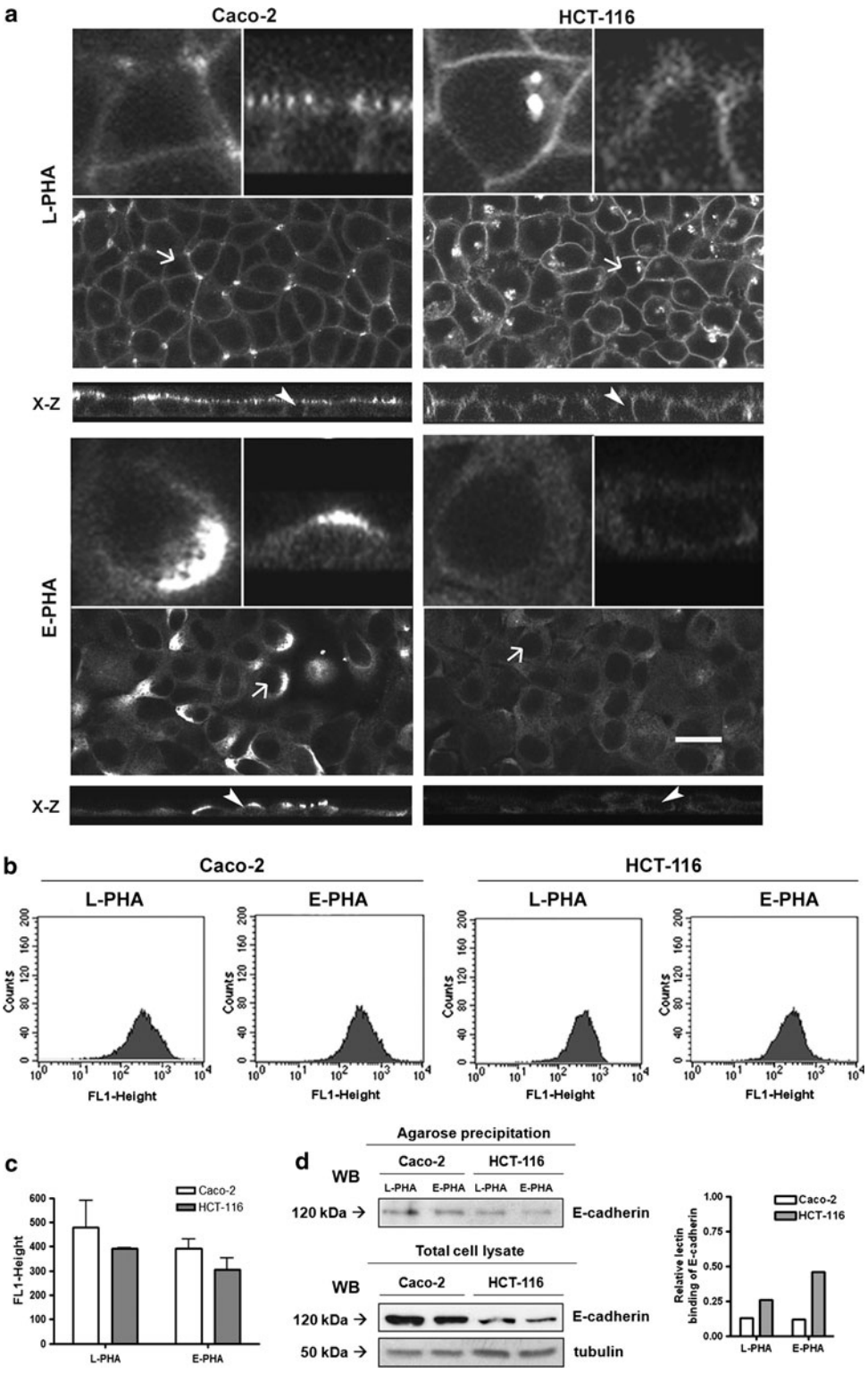

Fig. 2 E-cadherin from unstable AJs shows an increase in the expression of glycans that react with E-PHA and L-PHA **a** Staining patterns of E-PHA and L-PHA in Caco-2 and HCT-116 cells. Cell monolayers were grown on glass coverslips and labeled with FITC-conjugated L-PHA and E-PHA. Representative confocal microscopy images show the staining pattern of E-PHA and L-PHA. The *arrows* and *arrowheads* indicate the cells with magnified images. *Bar* = 20 μm. **b**, **c** Cell-surface labeling of FITC-conjugated L-PHA and E-PHA in Caco-2 and HCT-116 cells. After incubating cells with FITC-conjugated E-PHA (**b**) or L-PHA (**c**), the labeling on the cell surface was analyzed by flow cytometry, and fluorescence histograms were created with Cell Quest software. Unstained cells were used as controls. The bar graph shows the result of three independent experiments. **d** Differential E-cadherin glycosylation in Caco-2 and HCT-116 cells. After cell lysis, lectins were precipitated with agarose-conjugated E-PHA and L-PHA, and western blot analysis of E-cadherin was performed. Lectin binding of E-cadherin was normalized to the amount of E-cadherin expressed in each cell line. The *bar* graph shows the relative amount of lectins binding to E-cadherin from one representative experiment

Treatment with tunicamycin induces E-cadherin-mediated cell–cell adhesion

Because E-cadherin is the principal protein of AJ and our results suggest the involvement of *N*-glycans with the stability of AJs in CRC cells, we evaluated the effects of two well-known inhibitors of *N*-glycan biosynthesis, swainsonine and tunicamycin, and then conducted a functional E-cadherin analysis. First, immunofluorescence analysis was performed to determine the subcellular

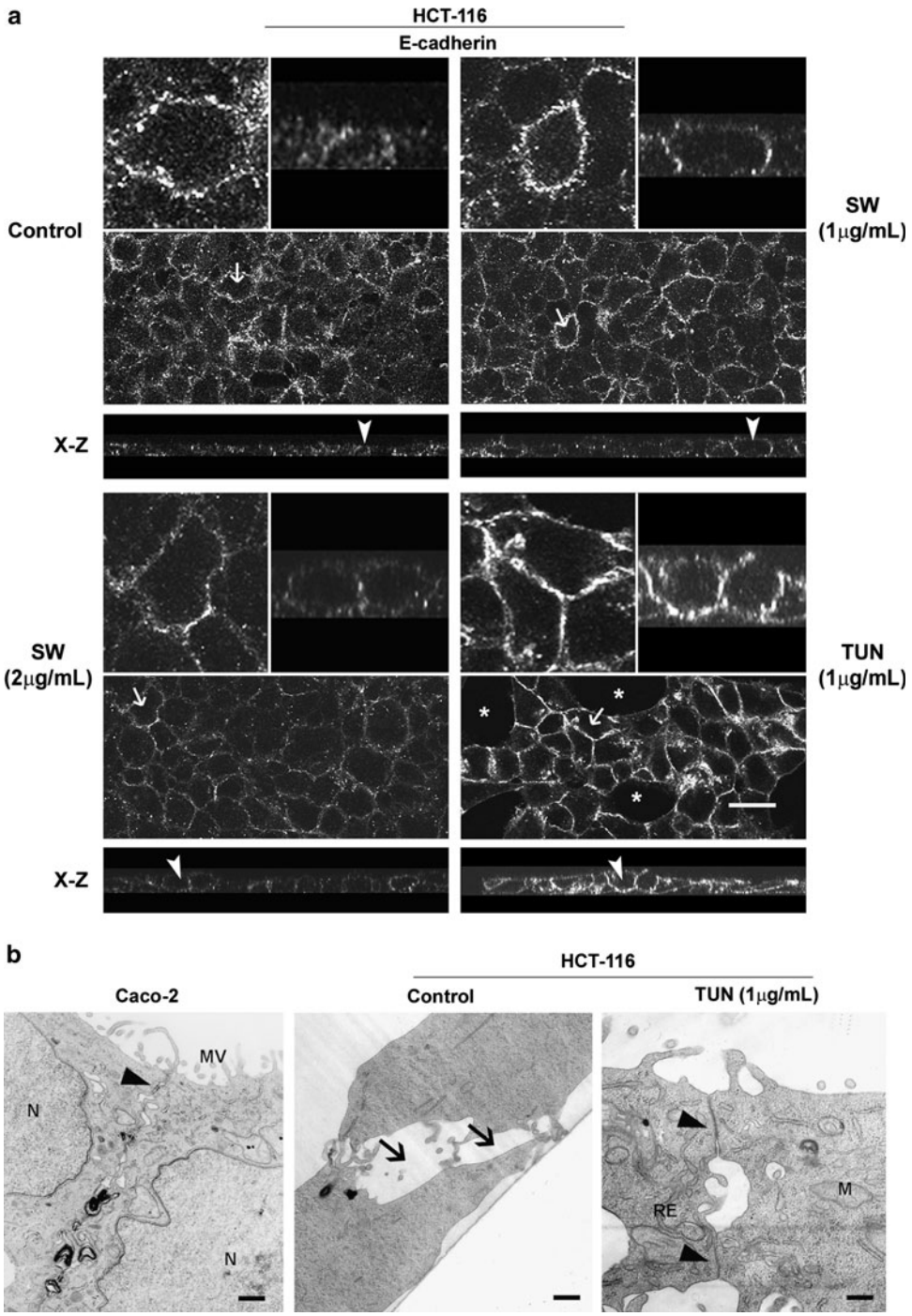

Fig. 3 Treatment with tunicamycin induces E-cadherin-mediated cell–cell adhesion. **a** Subcellular localization of E-cadherin in HCT-116 cells after treatment with tunicamycin and swainsonine. After reaching 80% confluence, cells were treated with tunicamycin and swainsonine for 24 h. Representative confocal microscopy images show the subcellular distribution of E-cadherin after treatment. On the superior part of the *panels*, *arrows* and *arrowheads* indicate magnified images at the X–Y and Z–Y plane, respectively. *Bar*: 20 μm. **b** Ultrastructural analysis of cell–cell contacts in Caco-2 and HCT-116 cells. Cells were left untreated or were treated as described earlier before being processed for analysis by transmission electron microscopy. Representative images show that untreated Caco-2 cells present a defined apical junctional complex (*arrowheads*) and that HCT-116 cells have wide intercellular areas, which indicate the absence of a functional apical junctional complex (*arrows*). Tunicamycin treatment induced tight formation of cell–cell contacts in HCT-116 cells. *M* mitochondria, *ER* endoplasmic reticulum, *N* nucleus, *MV* microvillus, *SW* swainsonine, *TUN* tunicamycin. *Bar* = 3 μm

localization of E-cadherin in undifferentiated HCT-116 cells after drug treatments. As shown in Fig. 3a, tunicamycin reduced the cytoplasmic E-cadherin levels and increased E-cadherin at the cell–cell contact regions. Swainsonine treatment apparently did not alter E-cadherin localization, which displayed an intercellular labeling pattern similar to that in control cells (Fig. 3a). Treatment of differentiated Caco-2 cells with swainsonine or tunicamycin did not affect the subcellular localization of E-cadherin (data not shown). We used transmission electron microscopy to analyze the effects of tunicamycin treatment on the cell–cell contact region. As shown in Fig. 3b, untreated Caco-2 cells, which have stable AJs, present a well-defined apical junctional complex characteristic of a polarized and differentiated phenotype. On the other hand, untreated HCT-116 cells exhibit a non-polarized phenotype and the absence of a defined apical junctional complex; after tunicamycin treatment, however, these cells developed

tight cell–cell contacts. This finding corroborates the results observed by immunofluorescence (Fig. 3b). Treating HCT-116 cells with swainsonine did not change their undifferentiated phenotype (data not shown). Collectively, these results suggest that pharmacological inhibition of *N*-glycan biosynthesis could interfere with the subcellular localization of E-cadherin and induce a differentiated-like phenotype in undifferentiated CRC cells.

E-cadherin-mediated cell–cell adhesion induced by tunicamycin is disrupted by calcium depletion

To assess the functionality of E-cadherin, we evaluated the amount of actin cytoskeleton-associated E-cadherin using a calcium depletion technique and Triton X-100 solubility criteria [31]. Calcium depletion is a well-known method of inducing E-cadherin-mediated disruption of cell–cell adhesion [10]. Western blot analysis indicates that treatment with swainsonine did not alter the expression of E-cadherin or its association with the actin cytoskeleton in Caco-2 cells (Fig. 4a, b) or in HCT-116 cells (Fig. 4c, d). However, tunicamycin treatment of HCT-116 cells induced a significant increase ($P < 0.05$) in actin cytoskeleton-associated E-cadherin, which was disrupted by calcium depletion (Fig. 4e). Corroborating this result, confocal microscopy images show an increase in cytoplasmic E-cadherin after calcium depletion, compared with tunicamycin treatment alone (Fig. 4f). The presence of a band with lower molecular weight indicates a shift of E-cadherin mobility after treatment with tunicamycin in HCT-116 and Caco-2 cells (Fig. 4a–c). The more pronounced shift in HCT-116 cells suggests a more richly *N*-glycosylated E-cadherin in these cells, which supports the results of our E-cadherin glycosylation analysis by agarose–lectin precipitation (Fig. 2d). Collectively, these data show that treatment with tunicamycin induces a functional E-cadherin-mediated cell–cell adhesion in undifferentiated HCT-116 cells. Because tunicamycin inhibits *N*-glycan biosynthesis, these results suggest that in advanced stages of colorectal cancer, represented here by HCT-116 cells, alterations in *N*-glycan expression may interfere with the stability of AJs.

Tunicamycin inhibits cell proliferation but does not induce apoptosis in undifferentiated HCT-116 cells

It is well known that homotypic ligation of E-cadherin induces signaling events associated with the inhibition of cell growth and that increased cell growth is an important hallmark of the tumor phenotype [32, 33]. In Figs. 3a and 4f, we observed free-cells regions on the HCT-116 cell culture area concomitantly to the E-cadherin recruitment at the cell–cell contact regions induced by tunicamycin treatment. Thus, we decided to perform subsequent experiments to assess cell proliferation and apoptosis after treatment with *N*-glycosylation inhibitors. Figure 5a shows that treatment with tunicamycin induced a significant decrease in cell proliferation after 18 and 24 h ($P < 0.05$), but treatment with swainsonine at 1 μg/ml and 2 μg/ml had no effect. This finding is consistent with the differentiated-like phenotype induced in HCT-116 cells treated with tunicamycin (Fig. 3a, b). Given that inhibition of *N*-glycosylation can lead to apoptosis from endoplasmic reticulum stress [34], we investigated whether our treatments (24 h) induced apoptosis. We found that neither swainsonine nor tunicamycin triggered apoptosis in undifferentiated HCT-116 cells (Fig. 5b). Collectively, these results show that the inhibition of *N*-glycan biosynthesis by tunicamycin not only induced a functional E-cadherin-mediated cell–cell adhesion but also reduced cell proliferation without causing apoptosis. Our findings therefore support the idea that tunicamycin induces a differentiated-like phenotype.

Discussion

Aberrant glycosylation has been associated with the loss of cell–cell adhesion, which constitutes a hallmark of tumor progression in epithelia [35, 36]. The cell lines used in this study represent two different stages of CRC progression. Although both are derived from malignant tumors, Caco-2 has a differentiated phenotype with a moderate metastatic potential, and HCT-116 has an undifferentiated phenotype with a high metastatic potential [25–27]. Here, in a correlative approach, we demonstrated that these cells exhibit opposite phenotypes in relation to AJ stability. Compared with Caco-2 cells, HCT-116 cells have lower levels of E-cadherin, α-catenin, and β-catenin associated with the actin cytoskeleton; this lack of association characterizes a more invasive phenotype [37].

Recent studies have emphasized that glycans that react with E-PHA and L-PHA play an important role in the development of migratory potential [36, 38, 39]. Thus, we evaluated whether Caco-2 and HCT-116 cells positively and differentially react with these lectins. Confocal microscopy showed that in HCT-116 cells, which have an unstable AJ phenotype, L-PHA was able to access the cell–cell contacts (Fig. 2a), which suggests that alteration of cell–cell adhesion may facilitate the ability of L-PHA to access its ligands in this area. Future studies should explore the functional role of endogenous lectins with similar specificity to L-PHA (e.g., galectin-3) to understand the real role of these molecules during CRC progression. Additionally, we speculate that at cell–cell contact regions, these glycans may act as a stereochemical barrier for the

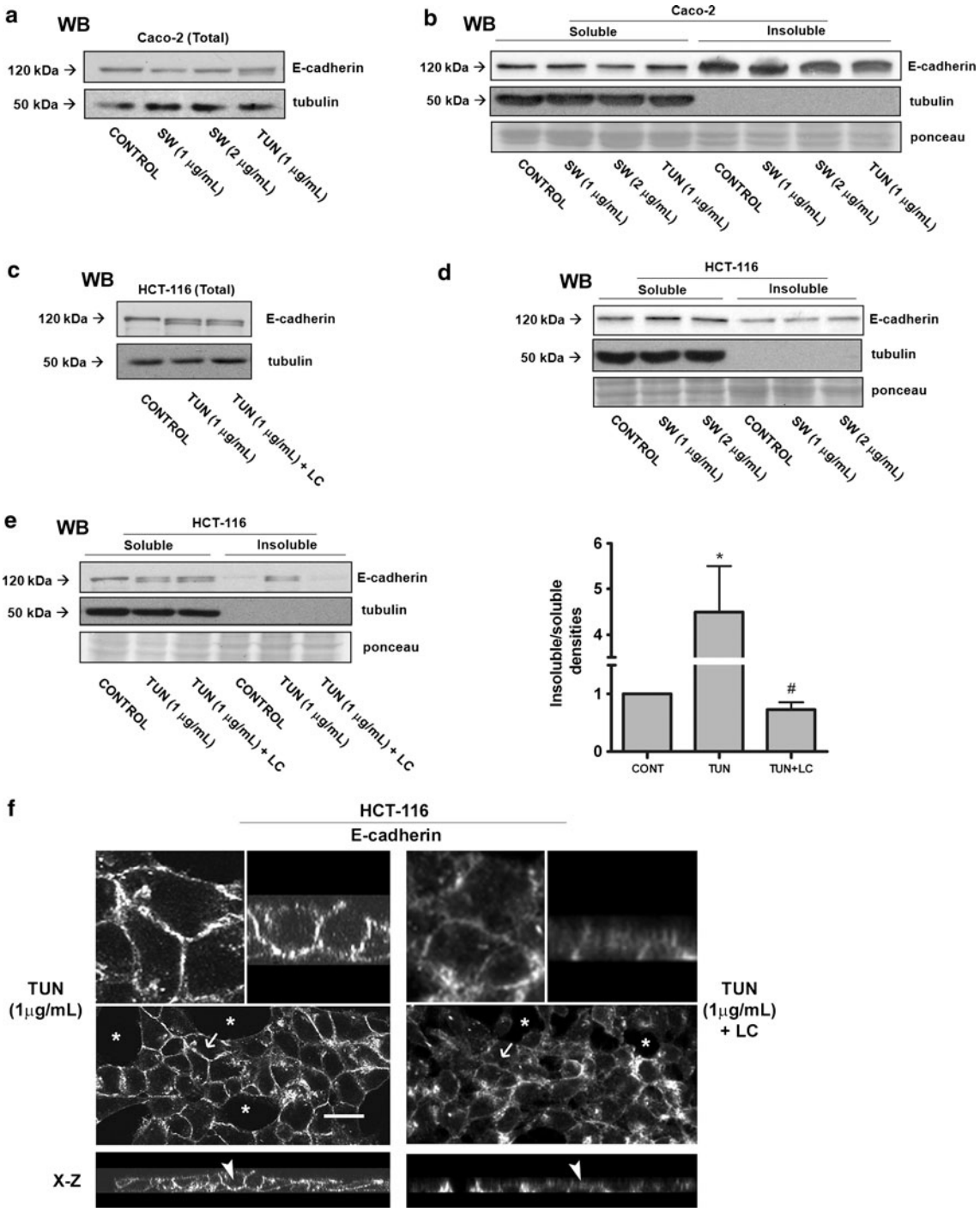

Fig. 4 E-cadherin-mediated cell–cell adhesion induced by tunicamycin is disrupted by calcium depletion. **a**, **b** E-cadherin expression and its association with the actin cytoskeleton in Caco-2 cells after treatment with swainsonine and tunicamycin. Cells were cultured and treated as indicated, and then the total lysate (**a**) and the Triton X-100-soluble and Triton X-100-insoluble fractions (**b**) were obtained and analyzed by western blot for E-cadherin. **c**, **d** E-cadherin expression and its association with the actin cytoskeleton in HCT-116 cells after treatment with swainsonine and tunicamycin. Cultured cells were untreated or treated as indicated, and then the total lysate (**c**) and the Triton X-100-soluble and Triton X-100-insoluble fractions (**d**) were obtained and analyzed by western blot for E-cadherin. **e** Functional E-cadherin analysis of HCT-116 cells after treatment with tunicamycin. A low calcium (LC) assay and preparation of the Triton X-100-insoluble and Triton X-100-soluble fractions were performed as described in the "Materials and methods" section. The *bar* graphs show the relative amount of E-cadherin associated with the cytoskeleton under the different assay conditions. *Error bars* indicate means +SEM ($n = 3$). * $P < 0.05$, # $P < 0.05$, ANOVA test. **f** Subcellular localization of E-cadherin in HCT-116 cells after treatment with tunicamycin and after calcium depletion. Cells were cultured and treated as described earlier and prepared for immunofluorescence analysis. Representative images obtained by confocal microscopy show the subcellular localization of E-cadherin after the treatments. *Bar* = 20 μm

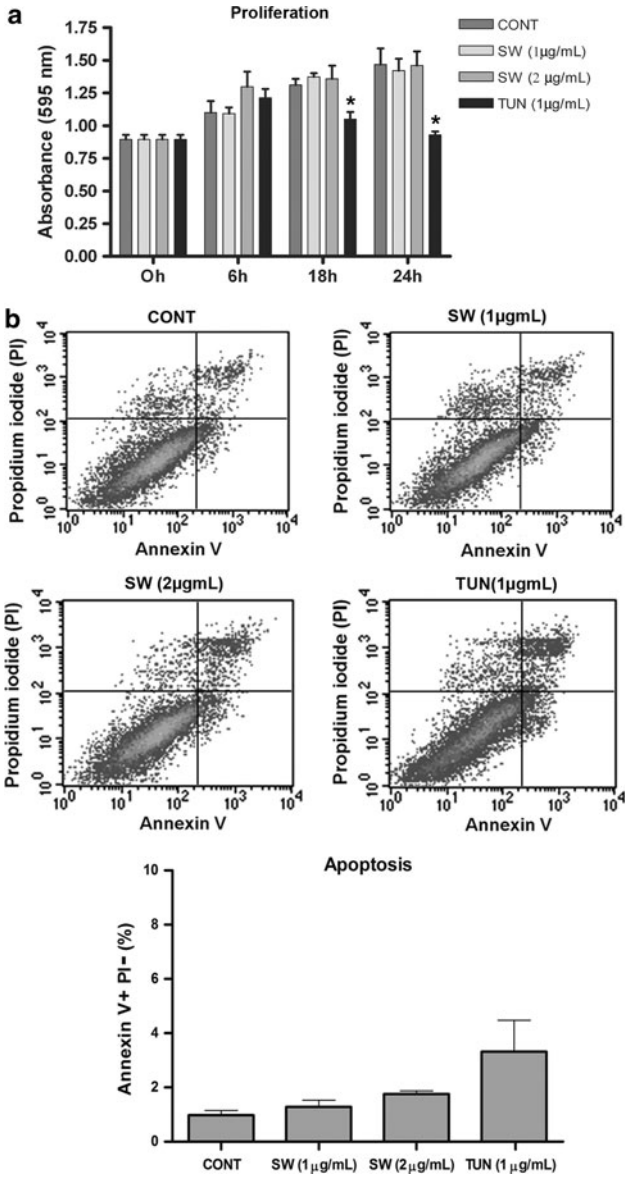

Fig. 5 Tunicamycin inhibits cell proliferation but does not induce apoptosis in undifferentiated HCT-116 cells. **a** Cell proliferation after treatment with swainsonine and tunicamycin. Cells (3×10^4) were cultured on 96-well plates, treated with the indicated drugs, and analyzed for cell proliferation 24 h later using the crystal violet technique. *Error bars* indicate means +SEM ($n = 3$). * $P < 0.05$; ANOVA test. **b** Apoptosis detection after treatment with swainsonine and tunicamycin. After 24 h of treatment with swainsonine and tunicamycin, apoptosis was assessed by cell staining with FITC-conjugated Annexin V and propidium iodide (PI). The *bar* graph represents the percentage of apoptotic cells (Annexin V = positive; PI = negative). *Error bars* indicate means + SEM ($n = 3$)

formation of stable and functional AJs; however, more studies are required to elucidate this issue. We observed an increased E-PHA staining pattern in Caco-2 cells (Fig. 2a). Because E-PHA recognizes products of the enzyme GnT-III (an *N*-acetylglucosaminyltransferase that catalyzes the formation of a bisecting GlcNAc structure in *N*-glycans, resulting in the suppression of metastasis), which cannot be used as substrates for the GnT-V enzyme (an *N*-acetylglucosaminyltransferase that catalyzes the addition of β-1,6-GlcNAc branching of N-glycans, which contributes to metastasis) [38], it is possible that the expression of GnT-III is higher in Caco-2 cells than in HCT-116 cells. This possibility supports the role of the GnT-III as a repressor of AJ disruption [39].

AJs are dynamic structures that undergo changes in molecular composition; therefore, we compared the E-cadherin glycosylation pattern using Caco-2 and HCT-116 cells, two models of AJ stability. Interestingly, our results demonstrated that the E-cadherin in undifferentiated HCT-116 cells had higher levels of complex-type *N*-glycans recognized by L-PHA and E-PHA than did Caco-2 cells. Our results indicate that this protein could be hyperglycosylated. In addition, the higher shift in E-cadherin mobility after treatment with tunicamycin (Fig. 4a–c) suggests that the E-cadherin in HCT-116 cells is more richly *N*-glycosylated than that in Caco-2 cells. Human E-cadherin has four potential *N*-glycosylation sites, which can be differentially glycosylated or unglycosylated [40]. Curiously, the E-cadherin in both cell lines could be modified by *N*-glycans that react with L-PHA and E-PHA. Thus, even in the Caco-2 cell line, which has stable and functional AJs, E-cadherin appears to possess complex-type *N*-glycans, not just the high-mannose glycans or the hybrids, that exist in the stable AJs of MDCK cells [17]. In studies of the basolateral membrane fractions of MDCK cells with stable AJs, it was demonstrated that after treatment with PNGaseF (an amidase that cleaves most *N*-glycans, including those with complex structures), the molecular weight of E-cadherin was lower than after treatment with EndoH (an endoglycosidase that preferentially hydrolyses high-mannose *N*-glycans) [41]. These results demonstrate that in other cells with stable AJs, E-cadherin can exhibit complex-type *N*-glycans.

Our findings encouraged us to analyze the effects of *N*-glycosylation inhibitors on AJ functionality. Although swainsonine did not produce considerable morphological changes in HCT-116 cells, tunicamycin induced a functional E-cadherin-mediated cell–cell adhesion (Figs. 3 and 4). Previous studies have shown that swainsonine induces a tight cell–cell adhesion in MDCK cells, whereas tunicamycin promotes an increase in paracellular permeability [41]. HCT-116 cells at 24 h resist apoptosis after tunicamycin treatment (1 µg/ml), which may explain the apparent contradiction with our findings. We also observed that in Caco-2 cells, treatment with swainsonine or tunicamycin did not alter the levels of actin cytoskeleton-associated E-cadherin. Although the results of our lectin precipitation suggest the presence of complex-type E-cadherin-linked *N*-glycans in Caco-2 cells, it is unlikely that these glycans

interfered with the stability of AJs. It has been reported that in MDCK cells with stable AJs, an E-cadherin-linked *N*-glycan did not appear to regulate AJ stability, but this *N*-glycan appeared to be a high-mannose or hybrid type [17]. Although swainsonine did not affect HCT-116 cells, tunicamycin increased the levels of actin cytoskeleton-associated E-cadherin; we therefore conclude that undifferentiated CRC cells have at least one complex-type E-cadherin-linked *N*-glycan involved with the regulation of AJ stability. Previous studies have demonstrated that tunicamycin preserves intercellular junctions and cytoarchitecture and inhibits ATP-depletion-mediated E-cadherin degradation in renal epithelial cells [42]. In addition, it has also been demonstrated that partial inhibition of dolichol-P-dependent *N*-acetylglucosamine-1-phosphate-transferase reduces *N*-linked glycosylation of E-cadherin, thereby stabilizing AJs in cells derived from oral cancer [35]. Also, hypoglycosylated E-cadherin has been shown to promote tight junction assembly [18]. Hence, more studies are needed to elucidate the precise molecular mechanisms through which E-cadherin-linked *N*-glycans can modulate AJs stability, especially during CRC progression.

We also observed that treatment with tunicamycin inhibited the formation of a confluent monolayer, which could indicate cell death (Figs. 3, 4). We then determined whether this *N*-glycosylation inhibitor affected cell proliferation or apoptosis. It is well known that the *N*-glycosylation process participates in the folding of quality control of proteins synthesized via ER (endoplasmic reticulum) [43] and that the inhibition of this process by tunicamycin can lead to cell death, as observed in neuroblastoma cells [34]. Our results do not agree with these studies because tunicamycin inhibited cell proliferation and did not induce apoptosis in HCT-116 cells. In this context, two hypotheses should be considered: (a) Undifferentiated HCT-116 colon cancer cells may has some resistant to unfolded protein response, or (b) the inhibition of *N*-glycosylation with 1 μg/ml tunicamycin at 24 h is not complete; this partial inhibition could be confirmed by the presence of a 120-kDa E-cadherin band that appears with the lower-molecular-weight band after treatment with tunicamycin (Fig. 4a–c). In addition, our results with tunicamycin (reduced cell proliferation and E-cadherin-mediated AJ stability) corroborate the induction of a differentiated-like cell phenotype.

In conclusion, our results show for the first time that *N*-glycans participate in the loss of AJ stability in undifferentiated colorectal cancer cells. Our findings suggest that changes in the pattern of expression of E-cadherin-linked *N*-glycans promote the loss of cell–cell adhesion during CRC progression. Moreover, the present study raises the possibility that tunicamycin may be a promising chemotherapeutic agent in experimental models of CRC progression.

Acknowledgments This study was sponsored by Conselho Nacional de Desenvolvimento Cientifico e Tecnologico (CNPq), Coordenação de Aperfeiçoamento de Pessoal de Nível Superios (CAPES), Ministerio da Saúde—Brasil, and Fundação Carlos Chagas Filho de Amparo à Pesquisa do Estado de Rio de Janeiro (FAPERJ). We are grateful to the Programa de Cooperação INCA/FIOCRUZ for the use of its facility. This text was reviewed by American Journal Experts.

References

1. Parkin DM, Bray F, Ferlay J, Pisani P (2005) Global cancer statistics, 2002. CA Cancer J Clin 55(2):74–108
2. Instituto Nacional de Câncer (2009) Estimativa/2010: Incidência de câncer no Brasil. Instituto Nacional de Câncer, Rio de Janeiro
3. Vogelstein B, Kinzler KW (2001) The genetic basis for human cancer. McGraw-Hill, Toronto
4. Behrens J (1999) Cadherins and catenins: role in signal transduction and tumor progression. Cancer Metastasis Rev 18:15–30
5. Vogelmann R, Nelson WJ (2005) Fractionation of the epithelial apical junctional complex: reassessment of protein distributions in different substructures. Mol Biol Cell 16(2):701–716
6. Ebnet K (2008) Organization of multiprotein complexes at cell-cell junctions. Histochem Cell Biol 130:1–30
7. de Araújo WM, Vidal FC, de Souza WF, de Freitas Junior JC, de Souza W, Morgado-Diaz JA (2010) PI3K/Akt and GSK-3β prevents in a differential fashion the malignant phenotype of colorectal cancer cells. J Cancer Res Clin Oncol. doi:10.1007/s00432-010-0836-5
8. Chung GG, Provost E, Kielhorn EP, Charette LA, Smith BL, Rimm DL (2007) Tissue microarray analysis of beta-catenin in colorectal cancer shows nuclear phospho-beta-catenin is associated with a better prognosis. Clin Cancer Res 7(12):4013–4020
9. Brand S, Olszak T, Beigel F, Diebold J, Otte JM, Eichhorst ST, Göke B, Dambacher J (2006) Cell differentiation dependent expressed CCR6 mediates ERK-1/2, SAPK/JNK, and Akt signaling resulting in proliferation and migration of colorectal cancer cells. J Cell Biochem 97(4):709–723
10. Leve F, de Souza W, Morgado-Díaz JA (2008) Across-link between protein kinase A and Rho-Family GTPases signaling mediates cell-cell adhesion and actin cytoskeleton organization in epithelial cancer cells. JPET 327:777–788
11. Tanaka MN, Diaz BL, de Souza W, Morgado-Díaz JA (2008) Prostaglandin E2-EPI and EP2 receptor signaling promotes apical junctional complex disassembly of Caco-2 human colorectal cancer cells. BMC Cell Biol 9:63
12. De Albuquerque Garcia Redondo P, Nakamura CV, de Souza W, Morgado-Diaz JA (2004) Differential expression of sialic acid and N-acetylgalactosamine residues on the cell surface of intestinal epithelial cells according to normal or metastatic potential. J Histochem Cytochem 52(5):629–640
13. Pinho SS, Reis CA, Paredes J, Magalhães AM, Ferreira AC, Figueiredo J, Xiaogang W, Carneiro F, Gärtner F, Seruca F (2009) The role of N-acetylglucosaminyltransferase III and V in the post-transcriptional modifications of E-cadherin. Hum Mol Genet 18(14):2599–2608
14. Lagana A, Goetz JG, Cheung P, Raz A, Dennis JW, Nabi IR (2006) Galectin binding to Mgat5-modified N-Glycans regulates fibronectin matrix remodeling in tumor cells. Mol Cell Biol 26(8):3181–3193
15. Lickert H, Bauer A, Kemler R, Stappert J (2000) J Biol Chem 275:5090–5095
16. Zhu W, Leber B, Andrews DW (2001) Cytoplasmic *O*-glycosylation prevents cell surface transport of E-cadherin during apoptosis. EMBO J 20(21):5999–6007

17. Liwosz A, Lei T, Kukuruzinska MA (2006) N-glycosylation affects the molecular organization and stability of E-cadherin junctions. J Biol Chem 281(32):23138–23149
18. Nita-Lazar M, Rebustini I, Walker J, Kukuruzinska MA (2010) Hypoglycosylated E-cadherin promotes the assembly of tight junctions through the recruitment of PP2A to adherens junctions. Exp Cell Res 316(11):1871–1884
19. Pinho SS, Osório H, Nita-Lazar M, Gomes J, Lopes C, Gärtner F, Reis CA (2009) Role of E-cadherin N-glycosylation in a mammary tumor model. Biochem Biophys Res Commun 379:1091–1096
20. Elbein AD (1987) Inhibitors of the biosynthesis and processing of N-linked oligosaccharide chains. Annu Rev Biochem 56:497–534
21. Mahoney WC, Duksin D (1980) Separation of tunicamycin homologues by reversed-phase high-performance liquid chromatography. J Chromatogr Sci 198:506–510
22. Fuster MM, Esko JD (2005) The sweet and sour of cancer: glycan as novel therapeutic targets. Nat Rev Cancer 5:526–542
23. Maeder T (2002) Sweet medicines. Sci Am 287:40–47
24. Ling YH, Li T, Perez-Soler R, Haigentz M Jr (2009) Activation of ER stress and inhibition of EGFR N-glycosylation by tunicamycin enhances susceptibility of human non-small cell lung cancer cells to erlotinib. Cancer Chemother Pharmacol 64(3): 539–548
25. Chantret I, Barbat A, Dussaulx E, Brattain MG, Zweibaum A (1988) Epithelial polarity, villin expression, and enterocytic differentiation of cultured human colon carcinoma cells: a survey of twenty cell lines. Cancer Res 48:1936–1942
26. Bull AW, Steffensen KR, Leers J, Rafter JJ (2003) Activation of PPAR γ in colon tumor cell lines by oxidized metabolites of linoleic acid, endogenous ligands for PPAR γ. Carcinogenesis 24(11):1717–1722
27. Lenaerts K, Mariman E, Bouwman F, Renes J (2006) Glutamine regulates the expression of proteins with a potential health-promoting effect in human intestinal Caco-2 cells. Proteomics 6(8):2454–2464
28. Laemmli UK (1970) Cleavage of structural proteins during the assembly of the head of bacteriophage T4. Nature 227:680–685
29. Contessa JN, Bhojani MS, Freeze HH, Rehemtulla A, Lawrence TS (2008) Inhibition of N-linked glycosylation disrupts receptor tyrosine kinase signaling in tumor cells. Cancer Res 68(10): 3803–3809
30. Sancho E, Batlle E, Clevers H (2004) Signaling pathways in intestinal development and cancer. Annu Rev Cell Dev Biol 20:695–723
31. Hinck L, Näthke IS, Papkoff J, Nelson WJ (1994) Dynamics of cadherin/catenin complex formation: novel protein interactions and pathways of complex assembly. J Cell Biol 125(6):1327–1340
32. Perrais M, Chen X, Perez-Moreno M, Gumbiner BM (2007) E-cadherin homophilic ligation inhibits cell growth and epidermal growth factor receptor signaling independently of other cell interactions. Mol Biol Cell 18(6):2013–2025
33. Weinberg RA (2006) The biology of cancer. Garland Science, New York
34. Song L, De Sarno P, Jope RS (2002) Central role of glycogen synthase kinase-3beta in endoplasmic reticulum stress-induced caspase-3 activation. J Biol Chem 277(47):44701–44708
35. Nita-Lazar M, Noonan V, Rebustini I, Walker J, Menko AS, Kukuruzinska MA (2009) Overexpression of DPAGT1 leads to aberrant *N*-glycosylation of E-cadherin and cellular discohesion in oral cancer. Cancer Res 69(14):5673–5680
36. Granovsky M, Fata J, Pawling J, Muller WJ, Khokha R, Dennis JW (2000) Suppression of tumor growth and metastasis in Mgat5-deficient mice. Nat Med 6(3):306–312
37. Ilyas M, Tomlinson IPM, Rowan A, Pignatelli M, Bodmer WF (1997) β-Catenin mutations in cell lines established from human colorectal cancers. Proc Natl Acad Sci 94:10330–10334
38. Zhao Y, Nakagawa T, Itoh S, Inamori K, Isaji T, Kariya Y, Kondo A, Miyoshi E, Miyazaki K, Kawasaki N, Taniguchi N, Gu J (2006) N-acetylglucosaminyltransferase III antagonizes the effect of N-acetylglucosaminyltransferase V on alpha3beta1 integrin-mediated cell migration. J Biol Chem 281(43):32122–32130
39. Iijima J, Zhao Y, Isaji T, Kameyama A, Nakaya S, Wang X, Ihara H, Cheng X, Nakagawa T, Miyoshi E, Kondo A, Narimatsu H, Taniguchi N, Gu J (2006) Cell-Cell interaction-dependent regulation of N-Acetylglucosaminyltransferase III and the bisected *N*-Glycans in GE11 epithelial cells. J Biol Chem 281(19): 13038–13046
40. Zhao H, Liang Y, Xu Z, Wang L, Zhou F, Li Z, Jin J, Yang Y, Fang Z, Hu Y, Zhang L, Su J, Zha X (2007) N-glycosylation affects the adhesive function of E-Cadherin through modifying the composition of adherens junctions (AJs) in human breast carcinoma cell line MDA-MB-435. J Cell Biochem 104(1): 162–175
41. Vagin O, Tokhtaeva E, Iskandar Y, Eugenia S, Sachs G (2008) Inverse correlation between the extent of N-Glycan branching and intercellular adhesion in epithelia. J Biol Chem 283(4): 2192–2202
42. George SK, Meyer TN, Abdeen O, Bush KT, Nigam SK (2004) Tunicamycin preserves intercellular junctions, cytoarchitecture, and cell-substratum interactions in ATP-depleted epithelial cells. Biochem Biophys Res Commun 10;322(1):223–231
43. Römisch K (2005) Endoplasmic reticulum-associated degradation. Rev Cell Dev Biol 21:435–456